Application of the $E - \epsilon$ Turbulence Closure Model to the Neutral and Stable Atmospheric Boundary Layer

P. G. DUYNKERKE

Free University, Amsterdam, The Netherlands

(Manuscript received 6 April 1987, in final form 19 August 1987)

ABSTRACT

In the $E - \epsilon$ turbulence model an eddy-exchange coefficient is evaluated from the turbulent kinetic energy E and viscous dissipation ϵ. In this study we will apply the $E - \epsilon$ model to the stable and neutral atmospheric boundary layer. A discussion is given on the equation for ϵ, which terms should be included and how we have evaluated the constants. Constant cooling rate results for the stable atmospheric boundary layer are compared with a second-order closure study. For the neutral atmospheric boundary layer a comparison is made with observations, large-eddy simulations and a second-order closure study. It is shown that a small stability effect can change the neutral atmospheric boundary layer quite drastically, and therefore, it will be difficult to observe a neutral boundary layer in the atmosphere.

1. Introduction

In this study we will apply the $E - \epsilon$ model, in which an eddy-exchange coefficient is evaluated from the turbulent kinetic energy E and the viscous dissipation ϵ, to the stable and neutral atmospheric boundary layer (ABL). The use of the $E - \epsilon$ model in engineering flows is now quite standard (Rodi, 1980). This popularity raises the question whether it could also be used for modeling the ABL, especially for flows in which the length scale cannot be prescribed in advance; for instance, under circumstances in which there are internal production processes of turbulent kinetic energy in the boundary layer, such as phase changes, radiative heating and radiative cooling in clouds (Duynkerke and Driedonks, 1987). Another application of the $E - \epsilon$ model is the flow over irregular terrain, in which a length scale is no longer determined by local (surface) characteristics (Rao et al., 1974; Beljaars et al., 1983).

In higher-order closure studies the use of the ϵ-equation has also become standard (Wyngaard et al., 1974; Zeman and Lumley, 1979; André et al., 1979). However, very little new insight in the ϵ-equation has been gained since the early work of Harlow and Nakayama (1967). Besides the frequent use of an ϵ-equation in higher-order closure studies we are aware of only a few applications of the $E - \epsilon$ model to atmospheric boundary-layer problems (Lee and Kao, 1979; Mason and Sykes, 1980; Detering and Etling, 1985a,b).

Lee and Kao (1979) combined the equations for E and ϵ to derive an equation for the eddy-exchange coefficient K. The constants used in this equation for K can be directly calculated from the constants used in the equation for E and ϵ. However, Lee and Kao (1979) divided the constants, which they proposed for the ϵ-equation, by 25 before calculating the constants in the equation for K. The reason and implications of this change are not clear to us. Mason and Sykes (1980) studied the dynamics of large-scale, horizontal roll vortices in the neutral ABL with an $E - \epsilon$ model. They concluded that the model results were completely stable for all perturbations, due to the anomalous high eddy-exchange coefficient obtained with the $E - \epsilon$ model. Similar results (too large K) were obtained by Detering and Etling (1985a) while simulating the neutral ABL.

Detering and Etling (1985a) compared their model results for the neutral ABL with the "Leipzig Wind Profile" (Mildner, 1932; Lettau, 1950, 1957) and concluded that both the eddy-exchange coefficient and the boundary layer height were much too large. Therefore, Detering and Etling (1985a) modified the ϵ-equation by making one of the constants a function of lf/u_*, which is the ratio of a turbulent length scale (l) and the depth of the neutral ABL (u_*/f). Qualitatively, this is analogous to a diagnostic length scale formulation in which l is proportional to u_*/f (Blackadar, 1962). Therefore, we think there is no real advantage in using their prognostic equation for ϵ above a diagnostic length scale. Moreover, we will show that the "Leipzig Wind Profile", which Detering and Etling (1985a) used to tune their model for the neutral case, is not representative for the truly neutral ABL, but some stability effect must be important. This was already noticed by Lettau (1950): "In the same air mass, the 1400 UTC sounding at the aerological station Lin-

Corresponding author address: P. G. Duynkerke, Royal Netherlands Meteorological Institute, P.O. Box 201, 3730 AE de Bilt, The Netherlands.

© 1988 American Meteorological Society

Unauthenticated | Downloaded 08/14/22 10:33 AM UTC

denberg (less than 100 miles from Leipzig) showed a rather uniform lapse rate of −0.65°C/100 m in the layer under consideration, which corresponds to an increase of potential temperature of 0.35°C/100 m."

Recently, Nicholls (1985) presented an observational study of the Ekman layer over sea during the Joint Air–Sea Interaction Experiment. The conditions were described as near neutral and barotropic. Nicholls (1985) concluded that in the absence of a low level inversion a well-mixed Ekman layer is observed on each occasion, which is limited to a height of $0.2u_*/f$.

Model simulations of the truly neutral ABL have been made by Deardorff (1972), Wyngaard et al. (1974) and Mason and Thomson (1986). Deardorff (1972) presented model results of a large-eddy simulation of the neutral ABL. He made two model runs, with model top at $0.45u_*/f$, and u_*/f, respectively. From the results of Deardorff (1972) it is clear that the height of the neutral ABL is somewhere between $0.45u_*/f$ and u_*/f. However, most of the results he presents are for the run with the lower model top and therefore these data cannot be trusted completely. Wyngaard et al. (1974) used a second-order closure model to simulate the neutral ABL and obtained a boundary layer height of $0.7u_*/f$. Recently, Mason and Thomson (1986) made a very detailed study of the neutral ABL with their large-eddy model; they found a boundary layer height of about $0.6u_*/f$ (their B10 case) for the neutral ABL.

The observational data (Lettau, 1950; Nicholls, 1985) thus show a boundary layer height of about $0.2u_*/f$, whereas the model results (Deardorff, 1972; Wyngaard et al., 1974; Mason and Thomson, 1986) show a boundary layer height of about $0.6u_*/f$. We will take the model results of Deardorff (1972), Wyngaard et al. (1974) and Mason and Thomson (1986) as representative for the truly neutral ABL, and with these data we will compare our model results for the neutral ABL (section 3b1). As noticed already by Lettau (1950) and Nicholls (1985) it will be difficult to observe this truly neutral boundary layer in the atmosphere. The differences between the experimental results in the near-neutral ABL and the theoretical solution of the truly neutral ABL reflects the presence of a weakly stable layer above the mixed layer in the observations. For instance, the potential temperature profiles presented by Nicholls (1982) show a neutral profile up to a certain height with a stable potential temperature gradient of 1 to 2 K km^{-1} aloft.

In order to reproduce the "Leipzig Wind Profile" and the observations of Nicholls (1985) we have initialized the model with a stable potential temperature gradient of 1 and 2 K km^{-1}, respectively. The model was run for 24 hours while the surface heat flux was kept zero. At the end of the simulation a neutral layer had formed up to a certain height, with a stable lapse rate above. In section 3b2 we have compared these model results with the observational data of Lettau (1950) and Nicholls (1982, 1985). Before using our model under conditions with arbitrary stratification we will first compare our model results with the model results of Wyngaard (1975) and Brost and Wyngaard (1978, 1979) on the stable ABL (section 3a).

2. Model description

In this section we will discuss the model, which is used in a one-dimensional horizontally homogeneous version. The ensemble-averaged equations for the horizontal velocities and the potential temperature are given in section 2a. In these equations the vertical velocity has been set equal to zero. The $E-\epsilon$ model is introduced in section 2a1, in which a full discussion is given on the equation for the viscous dissipation (ϵ).

In section 2a2 we show how we have determined the constants in the turbulence closure. Finally, section 2b gives details on the boundary conditions used.

a. Governing equations

We consider a horizontally homogeneous flow, with the mean velocities (u, v) in the (x, y) direction and mean potential temperature θ governed by

$$\frac{\partial u}{\partial t} = -\frac{\partial \overline{u'w'}}{\partial z} + f(v - v_g), \tag{1a}$$

$$\frac{\partial v}{\partial t} = -\frac{\partial \overline{v'w'}}{\partial z} - f(u - u_g), \tag{1b}$$

$$\frac{\partial \theta}{\partial t} = -\frac{\partial \overline{w'\theta'}}{\partial z}. \tag{1c}$$

Here f is the Coriolis parameter, (u_g, v_g) the geostrophic wind in the (x, y) direction, and primed quantities denote turbulent fluctuations.

1) TURBULENCE CLOSURE

For the fluxes in Eq. (1) a gradient transfer approach is taken:

$$-\overline{u'w'} = K\frac{\partial u}{\partial z}, \tag{2a}$$

$$-\overline{v'w'} = K\frac{\partial v}{\partial z}, \tag{2b}$$

$$-\overline{w'\theta'} = K\frac{\partial \theta}{\partial z}. \tag{2c}$$

The closure problem is now shifted to determining the distribution of K. In this paper the exchange coefficient will be determined from the turbulent kinetic energy (E) and the viscous dissipation of turbulent kinetic energy (ϵ) as

$$K = c_\mu E^2/\epsilon \tag{3}$$

in which c_μ is a constant and both E and ϵ have to be

Unauthenticated | Downloaded 08/14/22 10:33 AM UTC

determined from their modeled equations. This turbulence closure is called the $E-\epsilon$ model.

The turbulent kinetic energy equation in one-dimensional form reads

$$\frac{\partial E}{\partial t} = \underbrace{-\overline{u'w'}\frac{\partial u}{\partial z} - \overline{v'w'}\frac{\partial v}{\partial z}}_{S} + \underbrace{\frac{g}{\theta_0}\overline{w'\theta'}}_{B} \underbrace{-\frac{\partial}{\partial z}\left(\overline{w'E'} + \frac{\overline{p'w'}}{\rho_0}\right)}_{T} - \underbrace{\epsilon}_{D}, \quad (4)$$

in which p is the pressure. The momentum flux and heat flux are closed by (2). The transport term in (4) is modeled as

$$-\left(\overline{w'E'} + \frac{\overline{p'w'}}{\rho_0}\right) = \frac{K}{\sigma_E}\frac{\partial E}{\partial z}, \quad (5)$$

in which σ_E is the turbulent Prandtl number for E.

The equation for ϵ is the most difficult to model. At high Reynolds number ϵ is equal to the kinematic viscosity times the mean-square vorticity fluctuations ($\overline{\omega_i'\omega_i'}$). Tennekes and Lumley (1972) show that at sufficiently high Reynolds numbers there is a balance between the generation of $\overline{\omega_i'\omega_i'}$ due to vortex stretching and the destruction of $\overline{\omega_i'\omega_i'}$ due to viscosity. The next terms in order are the rate of change, advection and turbulent transport of $\overline{\omega_i'\omega_i'}$. Other terms are of higher order and can be neglected.

The transport term in the ϵ-equation is modeled with the gradient assumption

$$-\overline{w'\epsilon'} = \frac{K}{\sigma_\epsilon}\frac{\partial \epsilon}{\partial z}, \quad (6)$$

in which σ_ϵ is the turbulent Prandtl number for ϵ. The generation and destruction in the ϵ-equation, which are the biggest terms, are the most difficult to model. However, as pointed out by Tennekes (1985), the spectral energy flux and therefore the dissipation rate is determined by the dynamics at the large-scale end of the spectrum. Thus, ϵ is determined by the terms which produce the TKE. This idea was also used by Lumley and Khajeh-Nouri (1974) to parameterize the generation and destruction terms in the ϵ-equation. Using their parameterization for the generation and destruction we get

$$\frac{\partial \epsilon}{\partial t} = -\frac{\partial}{\partial z}\overline{w'\epsilon'} + \frac{\epsilon}{E}(c_{1\epsilon}P - c_{2\epsilon}\epsilon), \quad (7)$$

in which P is the production of turbulent kinetic energy. In their second-order closure study Wyngaard et al. (1974) have applied (7) with success to the neutral and convective ABL by using for P

$$P = S + B, \quad \text{with} \quad c_{1\epsilon} = 1.5, \quad c_{2\epsilon} = 2.0, \quad (8a)$$

so that the term between brackets in (7) becomes

$$(c_{1\epsilon}P - c_{2\epsilon}\epsilon) = (1.5S + 1.5B - 2\epsilon). \quad (8b)$$

This will be called the standard ϵ-equation. Moreover, Wyngaard (1975) applied the ϵ-equation to the stable boundary layer; in that case he used

$$(c_{1\epsilon}P - c_{2\epsilon}\epsilon) = (1.75S + 0.5B + 1\frac{B^2}{\epsilon} - 2\epsilon). \quad (9)$$

In order to clarify the difference between (8) and (9) we have drawn the terms $(1.5B/\epsilon)$ and $(0.5B/\epsilon + B^2/\epsilon^2)$ as a function of B/ϵ in Fig. 1. Thus, if $B > 0$ the expressions are almost equivalent. However, for $B < 0$ the influence of the buoyancy term (B) on the production term (P) in (9) is small. Therefore, in the range of interest ($-0.25 < B/\epsilon < 1$), the quadratic form in B [Eq. (9)] can be approximated by max(0, B). This was already used by Duynkerke and Driedonks (1987). The buoyancy term is thus only included in P if it is really a production term and is set to zero if it is a destruction term.

From the results on the neutral ABL in section 3b we will see that the transport term also can be an important source term in the turbulent kinetic energy budget (Mason and Thomson, 1986). Moreover, from the results in section 3b1 and the results of Detering and Etling (1985) it is clear that (9) does not give the correct results for the neutral ABL. From this we concluded that the transport term (T) should also be included in P in (7). We did this analogous to the buoyancy term. As a result P reads

$$P = S + \max(0, B) + \max(0, T). \quad (10)$$

In the next section we will evaluate the values of the constants used in the turbulence closure.

2) EVALUATION OF CONSTANTS

In the neutral surface layer, the two largest terms in (4) are S and D. Thus $S = D$ is a reasonable assumption which with (2) and (3) gives $c_\mu = (u_*^2/E)^2$. Panofsky and Dutton (1984) give a list of estimates of the ratio

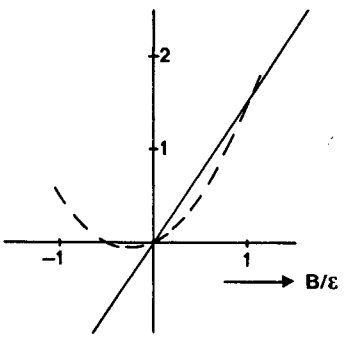

FIG. 1. The terms $(1.5B/\epsilon)$ (solid line) and $(0.5B/\epsilon + B^2/\epsilon^2)$ (dashed line) as a function of B/ϵ.

Unauthenticated | Downloaded 08/14/22 10:33 AM UTC

of standard deviations of velocity components to friction velocity, with an average of $E = 5.5u_*^2$; this gives $c_\mu = 0.033$.

In the equation for ϵ (7) three unknown constants appear: $c_{1\epsilon}$, $c_{2\epsilon}$ and σ_ϵ. The constant $c_{2\epsilon}$ is, as usual, based on the decay of grid turbulence. For the decay of grid turbulence Eqs. (4) and (7) reduce to

$$u\frac{\partial E}{\partial x} = -\epsilon, \quad u\frac{\partial \epsilon}{\partial x} = -c_{2\epsilon}\frac{\epsilon^2}{E}. \tag{11}$$

The exact solution of (11) is (Reynolds, 1974)

$$E/E_0 = \left(1 + \frac{x}{a}\right)^{-n}, \quad \frac{\epsilon}{\epsilon_0} = \left(1 + \frac{x}{a}\right)^{-(n+1)}, \tag{12}$$

with

$$n = \frac{1}{c_{2\epsilon} - 1}, \quad a = \frac{nuE_0}{\epsilon_0},$$

in which the index 0 indicates the value for $x = 0$. Measurements on the decay of neutral isotropic turbulence give values for n from 1 up to 1.4 (Monin and Yaglom, 1975). Reynolds (1974) proposed a simple model for the energy spectrum ($E(k)$) during the decay of isotropic turbulence. This model is only likely to work when the large-scale structure is devoid of any scales, i.e., when the large-scale energy is uniformly distributed over all wave vectors. This means that the spectrum tensor $\phi_{ii}(\mathbf{k})$ is the same at all $\mathbf{k}$ low wavenumbers and the three-dimensional energy spectrum function $E(k)$ is proportional to k^2. On this basis Reynolds (1974) got $n = 6/5$. This is a good average of all the experimental results (Monin and Yaglom, 1975). Therefore, we take $n = 6/5$ to fix $c_{2\epsilon}$, which gives with (12) $c_{2\epsilon} = 1.83$.

Next, we want to determine $c_{1\epsilon}$. Harris et al. (1977) and Tavoularis and Corrsin (1981) have studied a nearly homogeneous turbulent shear flow. A shear generator in a wind tunnel was used to create both turbulence and a uniform velocity gradient. The shear generator consisted of parallel channels of equal width with adjustable internal resistances. If no shear was present the turbulence would decay as described above. However, when a shear was applied there was continuous production of turbulent kinetic energy. This is described by Eqs. (4) and (7) as

$$u\frac{\partial E}{\partial x} = S - \epsilon, \quad u\frac{\partial \epsilon}{\partial x} = (c_{1\epsilon}S - c_{2\epsilon}\epsilon)\frac{\epsilon}{E}, \tag{13}$$

in which

$$S = c_\mu \frac{E^2}{\epsilon}\left(\frac{\partial u}{\partial z}\right)^2$$

and here $\partial u/\partial z$ is a constant. The full solution of (13) is rather complicated (Duynkerke and Nieuwstadt, 1988). Therefore, we will only give the solution for the ratio of E and ϵ:

$$e = E/\epsilon = \frac{\beta}{\alpha}\left\{\frac{c_0 e^{2\alpha\beta x} - 1}{1 + c_0 e^{2\alpha\beta x}}\right\}, \tag{14}$$

with

$$\beta^2 = \frac{c_{2\epsilon} - 1}{u}, \quad \alpha^2 = \frac{\hat{c}}{u}(c_{1\epsilon} - 1),$$

$$\hat{c} = c_\mu\left(\frac{\partial u}{\partial z}\right)^2, \quad c_0 = \frac{\beta/\alpha + e_0}{\beta/\alpha - e_0}.$$

For e_0 the value of e at $x = 0$. In the experimental results of Harris et al. (1977) and Tavoularis and Corrsin (1981) c_0 is large ($\sim$16), so that (14) reduces to

$$E/\epsilon = \beta/\alpha,$$

$$E/E_0 = e^{\gamma x}, \quad \epsilon/\epsilon_0 = e^{\gamma x}, \tag{15}$$

with

$$\gamma = \frac{\epsilon}{uE}\left(\frac{S}{\epsilon} - 1\right),$$

$$\frac{S}{\epsilon} = \frac{c_{2\epsilon} - 1}{c_{1\epsilon} - 1}.$$

This exponential increase (15) of E has also been found by Tavoularis (1985) using totally different arguments. From the experimental data of Harris et al. (1977) and Tavoularis and Corrsin (1981) we get that S/ϵ is a constant (independent of x) and equals 1.8. We had found already that $c_{2\epsilon} = 1.83$; this gives with (15) $c_{1\epsilon} = 1.46$.

Another way to tune the value of $c_{1\epsilon}$ is in a stably stratified flow in which the Richardson number has reached its critical value (Ri_c). In that case the transport terms and the rate of change in (4) and (7) can be neglected and thus reduce to

$$S + B - \epsilon = 0, \quad c_{1\epsilon}S - c_{2\epsilon}\epsilon = 0, \tag{16a}$$

which gives

$$c_{1\epsilon} = c_{2\epsilon}(1 - \mathrm{Ri}). \tag{16b}$$

From (16b) it is clear that the constants $c_{1\epsilon}$ and $c_{2\epsilon}$ determine the value of a critical Richardson number. With our values for $c_{1\epsilon}$ and $c_{2\epsilon}$ this gives $\mathrm{Ri}_c = 0.2$.

Finally the constant σ_ϵ in (6) has to be determined. In the neutral surface layer the transport term in the turbulent kinetic energy equation (4) is negligible, so that shear production equals viscous dissipation. Using this ($S = \epsilon$) in the equation for ϵ (7), in which the transport term is not negligible, one finds (Rodi, 1980)

$$\sigma_\epsilon = \frac{\kappa^2}{c_\mu^{1/2}(c_{2\epsilon} - c_{1\epsilon})}. \tag{17}$$

With the von Kármán constant $\kappa = 0.4$ this gives $\sigma_\epsilon = 2.38$. The only constant which is not fixed yet is σ_E, in (5). We take it as 1.

b. *Boundary conditions*

In order to calculate the turbulent fluxes near the surface we use the Monin–Obukhov similarity theory to relate the fluxes to the vertical gradients in the surface layer. For the similarity functions (ϕ) we took the func-

Unauthenticated | Downloaded 08/14/22 10:33 AM UTC

tion proposed by Dyer (1974). In the stable region the similarity function for momentum and heat are the same:

$$\phi = 1 + 5\frac{z}{L}. \tag{18}$$

The solution of the turbulent kinetic energy equation and the ϵ-equation requires specification of E and ϵ or their fluxes near the surface. We prescribed the values of E and ϵ at the first level above the surface (André et al., 1978):

$$E = c_\mu^{-1/2} u_*^2,$$

$$\epsilon = u_*^3 \left\{ \frac{\phi}{\kappa z} - \frac{1}{\kappa L} \right\}. \tag{19}$$

The surface boundary condition for ϵ is based on the fact that in the atmospheric boundary layer viscous dissipation balances shear production and buoyancy.

3. Results

a. *The stable ABL: Constant cooling rate results*

In this section we will study the quasi-stationary stable boundary layer. Here quasi-stationary means that the potential temperature is allowed to decrease with time but that other characteristic parameters (u_*, θ_*, L, etc.) are independent of time. This also means that the profiles of mean variables, fluxes and other turbulent quantities, made dimensionless with appropriate scaling parameters, should be independent with time.

Wyngaard (1975) integrated a full second-order turbulence model and demonstrated that the stable ABL could approach a steady state after 2–8 h, depending on the specified constant cooling rate at 1 m. He found that the boundary layer height (h) obeyed Zilitinkevich's similarity relation

$$h = d\left(\frac{u_* L}{f}\right)^{1/2}, \tag{20}$$

with $d = 0.22$. This low value of $d = 0.22$ compared to the more usual value of 0.4 (Garratt, 1982) is due to the constants specified in the ϵ-equation. The constants used by Wyngaard (1975) are given in Eq. (9). From the discussion given in section 2a2 it follows that these values specify a critical Richardson number of 1/8; this can also be seen in his Fig. 7. Nieuwstadt (1983) derived a formula for d as function of the von Kármán constant and the critical Richardson number

$$d^2 = (3)^{1/2} \kappa \, \mathrm{Ri}_c. \tag{21}$$

From (21) it can be seen that the too low value for the critical Richardson number (Wyngaard, 1975, used $\mathrm{Ri}_c = 1/8$) gives a too low value for d.

Brost and Wyngaard (1978, 1979) simplified the second-order closure model of Wyngaard (1975) considerably by neglecting time derivatives, Coriolis terms and triple correlations. Instead of using an equation for ϵ they parameterize ϵ as $E^{3/2}/l$, where they specify the turbulent length scale l. As noted by Fitzjarrald (1979) these simplified equations can be rewritten in the form of an eddy-exchange coefficient formulation. Brost and Wyngaard (1979) found that d varied from 0.37 to 0.51 for cooling rates from 0.2 to 6 K h^{-1}.

We generated four cases with our model by applying cooling rates of 0.2, 0.5, 1 and 2 K h^{-1} at the surface. This is somewhat different from Wyngaard (1975) and Brost and Wyngaard (1978, 1979) because they have applied the cooling rate at $z = 1$ m. As in Brost and Wyngaard (1979) we took $G = 10$ m s^{-1} and $z_0 = 0.01$ m. In Table 1 we compare the quasi-steady state results after 10 h for the four different cooling rates with the results of Brost and Wyngaard (1979).

In this study, as in Wyngaard (1975) and Brost and Wyngaard (1979), h is taken as the height at which the stress is 5% of its surface value. This definition of h is used because it is difficult to determine h from the potential temperature profile. From this definition of h we find that d varies between 0.43 and 0.45 and is thus nearly constant. Moreover our model results show nearly the same values of α (the angle between the surface wind and the geostrophic wind) and h/L as those of Brost and Wyngaard (1979). Because Brost and Wyngaard (1979) have used the flux-profile relations of Businger et al. (1971) and we have used the flux-profile relations of Dyer (1974) their values of u_*

TABLE 1. For 10 h after transition and different constant cooling rates, boundary layer depth h, Monin–Obukhov length L, friction velocity u_*, surface vertical potential temperature heat flux Q_0, cross isobar angle α, stability parameter h/L and the constant d in Zilitinkevich's Eq. (20).

	0.2 K h^{-1}		0.5 K h^{-1}		1 K h^{-1}		2 K h^{-1}	
	Present	BW (1979)	Present	BW (1979)	Present	BW (1979)	Present	BW (1979)
h	329	194	182	127	115	86	71	55
L	195	120	77	48	36	23	16	9.9
u_*	0.31	0.23	0.27	0.20	0.23	0.176	0.19	0.147
Q_0	−0.0112	−0.0084	−0.0190	−0.0139	−0.0251	−0.0189	−0.0305	−0.024
α	27	29	33	34	38	38	43	42
h/L	1.7	1.6	2.4	2.6	3.2	3.7	4.4	5.6
d	0.45	0.37	0.43	0.41	0.43	0.43	0.44	0.46

Unauthenticated | Downloaded 08/14/22 10:33 AM UTC

and Q_0 are approximately 25% lower than ours. As a result both the values of L and h we find are much higher. However, the Zilitinkevich relation (20) still holds very well, with an average value for d of 0.44.

Figure 2 shows the wind spiral, made dimensionless by u_*, after 10 h for a cooling rate of 1 K h^{-1}. In Fig. 3 we have plotted the temperature profiles for the four different cooling rates as a function of height. The temperature differences, made dimensionless with the temperature difference at the surface, as a function of z/h show that for the higher cooling rates the cooling is penetrating up to larger z/h values, due to the lower values of h/L. The temperature profile (1 K h^{-1}) presented by Brost and Wyngaard (1978) shows a very similar structure.

Next we will discuss some turbulence quantities. Figure 4 shows the turbulent kinetic energy as a function of height. This profile is similar to the profile observed in the neutral ABL (Fig. 10). In Fig. 5a we have compared our stress profiles with the stress profiles of Wyngaard (1975). It is not clear why the stresses of Wyngaard (1975) do not sum to 5% at $z = h$, because this is his definition of the boundary layer h. The heat flux profiles (Fig. 5b) show a slight curvature at the top of the boundary layer, analogous to the results of Brost and Wyngaard (1978), with a maximum cooling rate at the ground.

Brost and Wyngaard (1978) found that the profile of the eddy diffusivity for momentum is well represented by

$$\frac{K_m}{\kappa u_* h} = \frac{\frac{z}{h}\left(1 - \frac{z}{h}\right)^{1.5}}{1 + 4.7\left(\frac{z}{h}\right)\left(\frac{h}{L}\right)}, \tag{22}$$

whereas the ratio K_h/K_m averages about 1.2.

In Fig. 6 we have compared (22) with our model results which illustrates a good agreement between both results. In Fig. 7 we have shown the profile of the Richardson number, which shows that the Richardson number equals its critical value throughout almost the whole boundary layer; for $z/h > 1$ the Richardson number exceeds its critical value and near the surface $\mathrm{Ri} < \mathrm{Ri}_c$ due to the high shear production. This kind of behavior was already observed by Nieuwstadt (1983, 1984) and Garratt (1982).

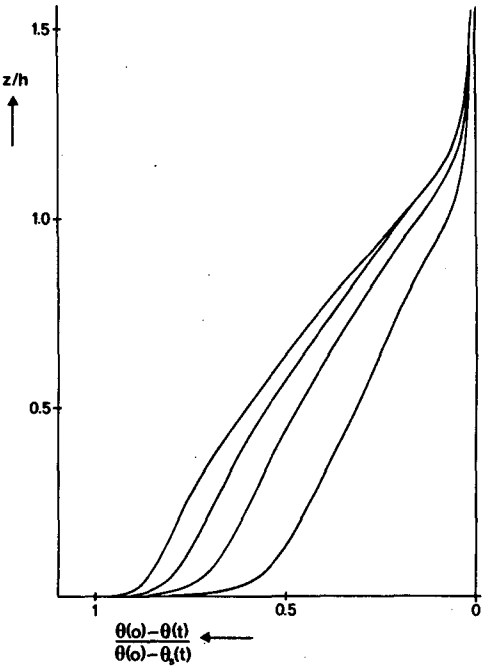

FIG. 3. For 10 h after transition the dimensionless temperature rofile as a function of z/h, from right to left, for a cooling rate of 0.2, 0.5, 1 and 2 K h^{-1}, respectively.

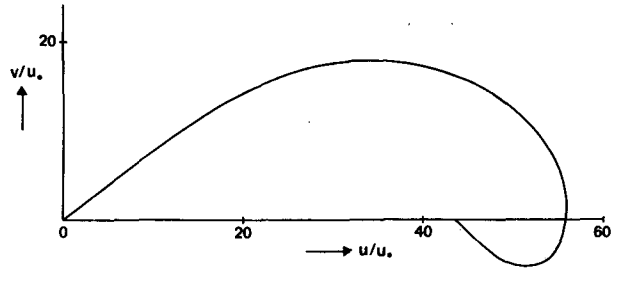

FIG. 2. The dimensionless wind spiral 10 h after transition, for a cooling rate of 1 K h^{-1}.

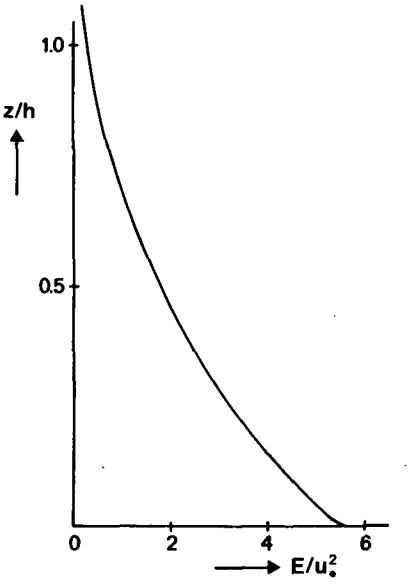

FIG. 4. The turbulent kinetic energy (E) as a function of height.

Unauthenticated | Downloaded 08/14/22 10:33 AM UTC

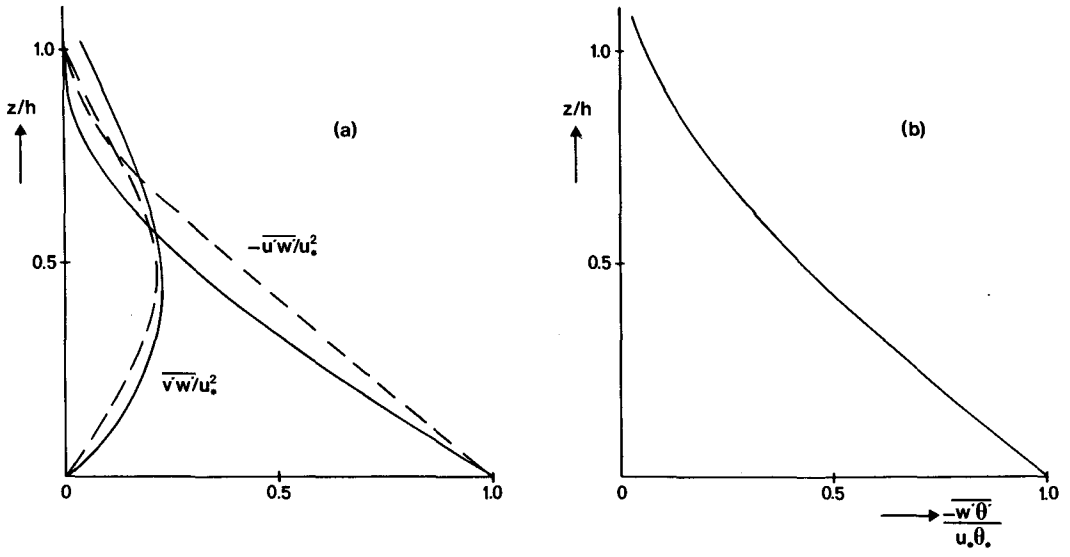

FIG. 5. The profiles of the (a) momentum flux and (b) heat flux as a function of height: our results (solid line), results of Wyngaard (1975) (dashed line).

We can conclude that with our $E - \epsilon$ model we can reproduce the results of Wyngaard (1975) and Brost and Wyngaard (1978, 1979) very well. Essential in obtaining these results is the critical Richardson behavior introduced in the ϵ-equation. This could be reached by including a term max(0, B) instead of B in the production term. Although something similar was already done by Wyngaard (1975), using a quadratic function

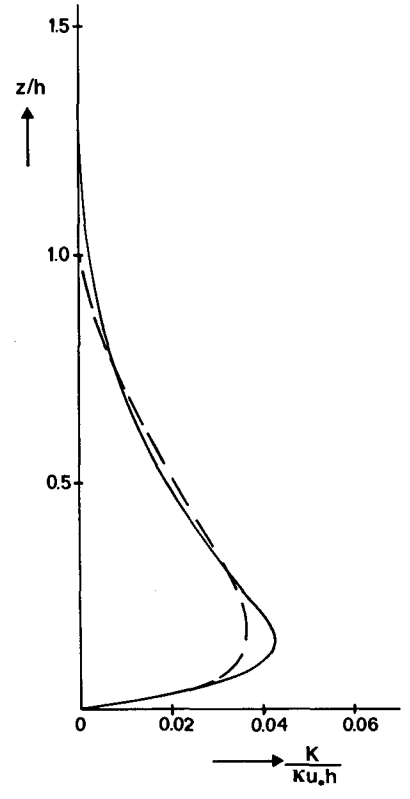

FIG. 6. Comparison of Brost and Wyngaard's (1978) (dashed) eddy diffusivity and our model results (solid).

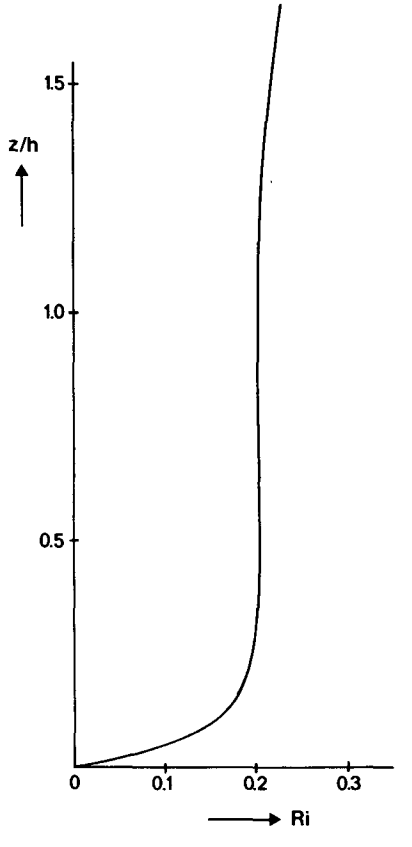

FIG. 7. Variation of the Richardson number with height.

Unauthenticated | Downloaded 08/14/22 10:33 AM UTC

in B (see section 2a), he did not explain the necessity of this clearly.

b. The neutral ABL

In the neutral ABL the heat flux is, by definition, identical to zero. In a model this condition can be easily satisfied. However, in this section we will demonstrate that in the atmosphere a boundary layer with neutral stratification can hardly ever be observed. Therefore, observational data presented as representative for the neutral ABL (Nicholls, 1985; "Leipzig Wind Profile") are in fact influenced by (a slightly stable) stratification.

In our model we have used a prognostic equation for the viscous dissipation ϵ, which is analogous to a prognostic equation for the turbulent length scale l. However, it is also possible to diagnose a length scale. For instance, based on observations Blackadar (1962) proposed a length scale as

$$l = 2.7 \times 10^{-4} G/f, \tag{23}$$

which is similar to the length scale used by Detering and Etling (1985a):

$$l = 6.3 \times 10^{-3} u_*/f. \tag{24}$$

However, prescribing a length scale with (23) or (24) means that the boundary layer height is determined by the value of the constant.

In order to circumvent this problem Detering and Etling (1985a) used an $E - \epsilon$ model for the neutral ABL. They modified the constant $c_{2\epsilon}$ [Eq. (7)] in such a way that the model results fit the "Leipzig Wind Profile". Detering and Etling (1985a) did this by making $c_{2\epsilon}$ a function of lf/u_*, with l proportional to $E^{3/2}/\epsilon$. It is clear that this modification is more or less the same as diagnosing a length scale by (24) and therefore, there is no real advantage in using the ϵ-equation above a diagnostic length scale (24).

In this section we will present model results for the truly neutral and near-neutral ABL over sea (Nicholls, 1985). We have taken $z_0 = 2 \times 10^{-4}$ m and $G = 10$ m s^{-1} and all the results shown are for a simulation time of 24 h. In section 3b1 we will compare our model results with the large-eddy simulations by Deardorff (1972) and Mason and Thomson (1986) and the higher-order closure study by Wyngaard et al. (1974) of the neutral ABL. In section 3b2 we will initialize the model with a stable potential temperature gradient of 1 and 2 K km^{-1} and set the surface heat flux to zero. The resulting profiles will be compared with the observational data of Nicholls (1982, 1985) and the "Leipzig Wind Profile" (Mildner, 1932; Lettau, 1950).

1) COMPARISON WITH MODEL RESULTS ON THE NEUTRAL ABL

Application of the standard $E - \epsilon$ model [Eq. (7)] to the neutral ABL gave the same unrealistic results as Detering and Etling (1985a) found. The eddy-exchange coefficient and the length scale increase linearly with height up to the model top, as shown in Figs. 8 and 9. In Fig. 8 we have also plotted the K-profiles of Wyngaard et al. (1974). We see that in the upper part of the boundary layer our eddy-exchange coefficients are much higher than those of Wyngaard et al. (1974). As a result, the boundary layer height extends up to the model top, which can be seen from the turbulent kinetic energy profile in Fig. 10. This boundary layer height is too high compared with the model results of Deardorff (1972), Mason and Thomson (1986) and Wyngaard et al. (1974), which are also shown in Fig. 10.

This discrepancy between our model results and the other model results is due to the fact that at the top of the neutral boundary layer the transport term is an important source term in the turbulent kinetic energy equation, whereas in the standard ϵ-equation the transport term as a source term is neglected. The fact that the transport term is important in the upper part of the neutral boundary layer can be seen from the TKE budget of the large-eddy simulation of Mason and Thomson (1986), which is shown in Fig. 11. In almost the whole neutral ABL the shear production and viscous dissipation are an order of magnitude larger than the transport term, except above $\sim 0.3u_*/f$ where the transport term assumes increasing importance. This gave us the idea to include the transport of TKE as a production term in the ϵ-equation (7). Analogous to the buoyancy term we only included it when the transport term was positive (10). However, from the simulation of the neutral and stable boundary layer no conclusion could be reached about what to do in regions in which the transport term is negative, because

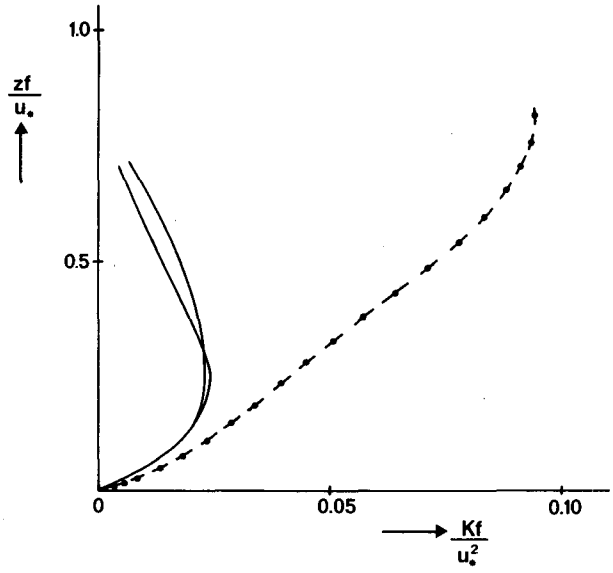

FIG. 8. Vertical distribution of eddy viscosity in the neutral atmospheric boundary layer for standard $E - \epsilon$ model (dashed) and the results of Wyngaard et al. (1974) (solid).

Unauthenticated | Downloaded 08/14/22 10:33 AM UTC

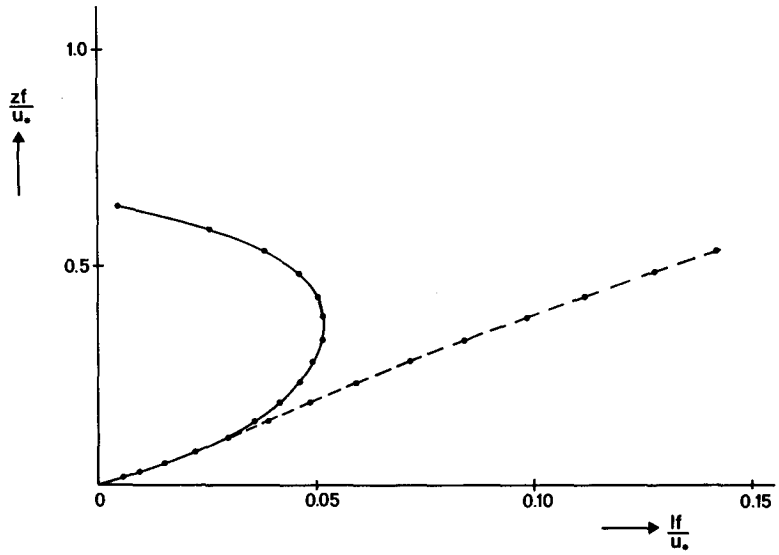

FIG. 9. The length scale as a function of height for the standard (dashed) and modified (solid) $E - \epsilon$ model.

in those regions the shear production and viscous dissipation were an order of magnitude larger.

We will now discuss the results of the modified $E - \epsilon$ model in which the transport term (T) has been included in the production term (P) in the ϵ-equation (7). In Fig. 10 we have compared the TKE profile with the other model results, the observations of Nicholls (1985) and measurements on a boundary layer in a wind tunnel (Hinze, 1975). Extensive measurements on turbulence quantities in the boundary layer of a wind tunnel have been made, many of which have been summarized by Hinze (1975). Because we expect some similarity between turbulence quantities in a wind tunnel boundary layer and the ABL, we have made some comparison, especially, in the case of quantities which cannot be so easily measured in the atmosphere. In order to do so we have set the boundary layer height in the wind tunnel equal to $0.5u_*/f$. We see that our turbulent kinetic energy profile is nearly identical to that of Deardorff (1972), Wyngaard et al. (1974) and

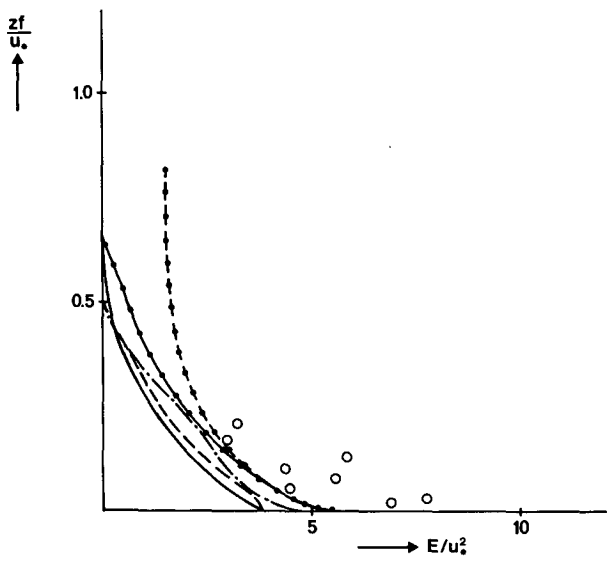

FIG. 10. The vertical profile of turbulent kinetic energy, neutral case: observations of Nicholls (1985) (○); standard $E - \epsilon$ (dashed with dot); modified $E - \epsilon$ (solid with dot); Deardorff (1972) (dashed); Wyngaard et al. (1974) (solid); Hinze (1975) (dot-dashed).

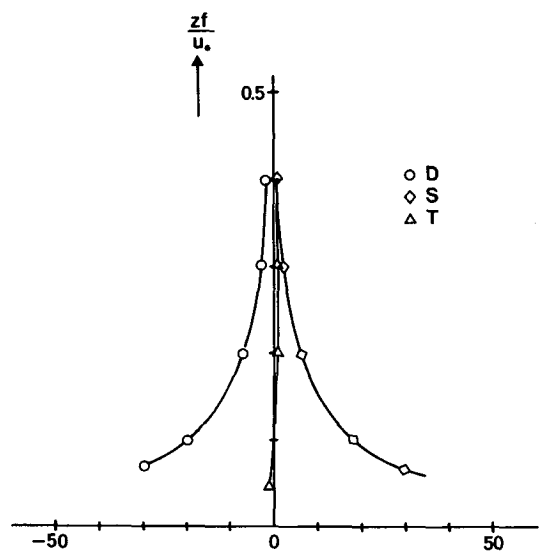

FIG. 11. Balance of terms in the turbulent kinetic energy equation for the neutral boundary layer (Mason and Thomson, 1986: B10 case).

Unauthenticated | Downloaded 08/14/22 10:33 AM UTC

the laboratory data (Hinze, 1975), whereas the values observed by Nicholls (1985) are somewhat higher. The higher values of the turbulent kinetic energy in the atmosphere might be a result of the fact that there is a significant contribution from larger scales ($\geq u_*/f$) as can be seen in the measured velocity spectra in Nicholls (1985).

In Fig. 12 we have shown the dimensionless wind profiles as a function of zf/u_*. We see that our results compare rather well with the profiles of Wyngaard et al. (1974). The profiles of Deardorff (1972) are somewhat different due to the too low model top used during his run ($z_t = 0.45u_*/f$). Here, we see that there is a big difference between the model results and observational data. As mentioned already, this is due to the fact that the observations do not represent a neutral ABL as can be seen from the observed temperature profiles of Nicholls (1982). This will be discussed further in the next section. In Fig. 13 we have compared the stress profiles with the observations of Nicholls (1985). We see that especially the resemblance in $\overline{v'w'}$ is very poor.

In Fig. 14 we have compared the computed eddy-exchange coefficient profiles with the profiles of Deardorff (1972), Wyngaard et al. (1974) and the laboratory data (Hinze, 1975). We see that the values agree rather well and moreover, the maxima show up at the same height. In Fig. 15 we have compared the computed TKE budget with the values measured by Nicholls (1985). We see that the shear production (S) and dissipation agree rather well, but the measured transport term (T) is an order of magnitude larger than the computed transport term. If we compare the TKE budget calculated with the $E - \epsilon$ model with the TKE budget of Mason and Thomson (1986) we see that the agreement is excellent. Moreover, from the TKE budget it is clear why it will be hard to observe a neutral boundary layer in the atmosphere. At about $0.25u_*/f$ the production of turbulent kinetic energy becomes small and therefore a weak stable stratification can make the turbulence die out. This will be discussed in the next section.

Before turning to the observations we will test the Rossby number similarity (Tennekes, 1973) of this model. According to this theory, the geostrophic drag coefficient (u_*/G) and the cross-isobar angle (α) should be functions of the surface Rossby number ($\mathrm{Ro} = G/fz_0$) only. We varied the Rossby number by varying z_0 and have plotted u_*/G and α as a function of Ro in Fig. 16. We have also shown the results of Mason and Thomson (1986) (B10 case) and Deardorff (1972). The results of Wyngaard et al. (1974) (for $\kappa = 0.4$) are not shown because they are nearly identical to those of Mason and Thomson (1986). If we compare the computed u_*/G and α (Fig. 16) with observational data (Tennekes, 1973) we see that the values of u_*/G agree rather well whereas the observed values of α are somewhat larger. We believe this is due to the sensitivity of the cross-isobar angle on stability and in the observational data some stability will be always important.

2) COMPARISON WITH OBSERVATIONS ON THE NEARLY NEUTRAL ABL

In section 3b1 we have shown that there is a difference between observational data on the near-neutral

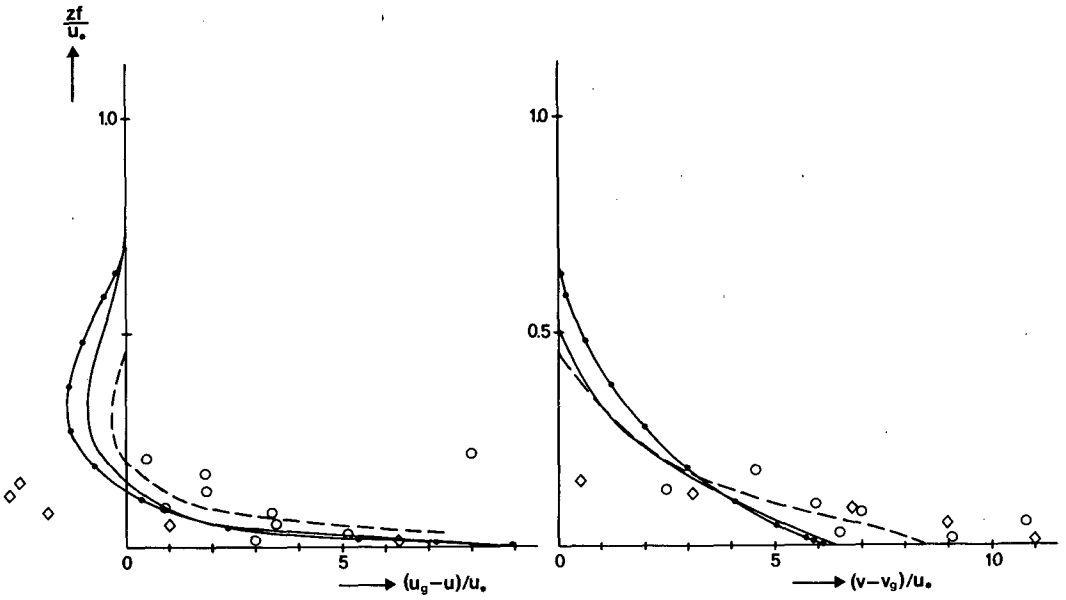

FIG. 12. Nondimensional wind defect profiles: Nicholls (1985) (○); Lettau (1950) (◇); modified $E - \epsilon$ (solid with dot); Deardorff (1972) (dashed); Wyngaard et al. (1974) (solid).

Unauthenticated | Downloaded 08/14/22 10:33 AM UTC

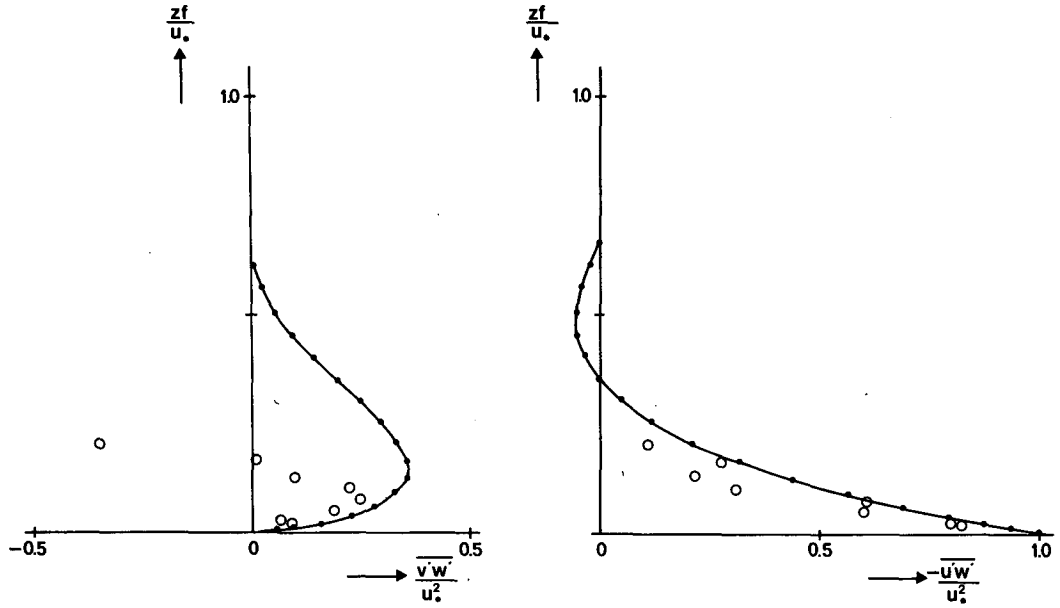

FIG. 13. Nondimensional momentum flux profiles: Nicholls (1985) (open circles); modified $E - \epsilon$ (solid line).

ABL and model results of the truly neutral ABL. Especially, there is a big difference between observed ($h \sim 0.2u_*/f$) and calculated ($h \sim 0.6u_*/f$) boundary layer height. This discrepancy can be directly explained by the TKE budget of the neutral ABL, as shown in Fig. 15. Above $\sim 0.25u_*/f$ the production term becomes small and in the real atmosphere a small stability will prevent the layer from being turbulent. The measured potential temperature profiles (Nicholls, 1982, 1985) show a neutral layer up to $z \sim 0.2u_*/f$ with a slightly stable region above (potential temperature gradient of 1 to 3 K km^{-1}). Thus the neutral boundary layer is inhibited to grow higher by a stable lapse rate aloft and this we will simulate in this section.

The model was initialized with a stable lapse rate of 1 and 2 K km^{-1}, respectively, as shown in Fig. 17. We have run the model for 24 hours during which the surface heat flux was set equal to zero. The final potential

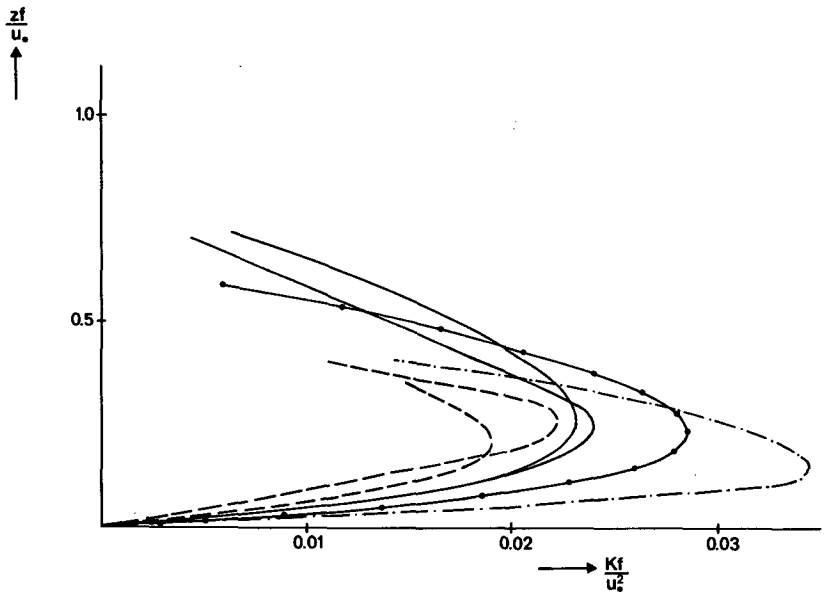

FIG. 14. Vertical distribution of eddy-exchange coefficient in the neutral boundary layer: Hinze (1975) (dot-dashed); modified $E - \epsilon$ (solid with dot); Deardorff (1972) (dashed); Wyngaard et al. (1974) (solid).

Unauthenticated | Downloaded 08/14/22 10:33 AM UTC

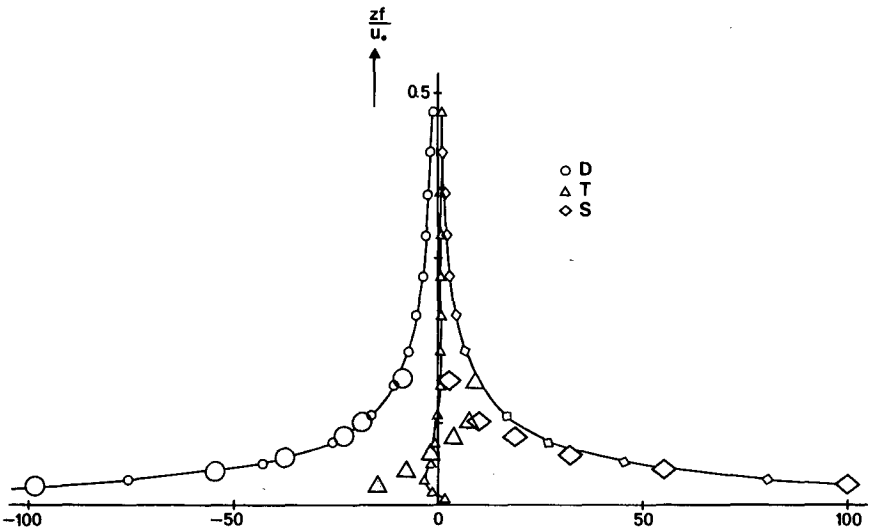

FIG. 15. Vertical profiles of the terms in the turbulent kinetic energy budget; large symbols, observational data of Nicholls (1985); small symbols connected with lines, modified $E - \epsilon$ model.

temperature profiles show a neutral layer up to $0.16u_*/f$ and $0.12u_*/f$, respectively. Above this neutral layer a slightly stable region is being formed. These vertical profiles of potential temperature are very similar to those observed by Nicholls (1982).

In Fig. 18 we have compared the calculated vertical velocity–defect profiles with the "Leipzig Wind Profile" (Lettau, 1950) and the data of Nicholls (1985). The model results give a value for the cross-isobar angle α of 11.4° and 12.7° for a stable lapse rate of 1 and 2 K km^{-1}, respectively. In the "Leipzig Wind Profile" α = 26.1° which is somewhat larger than in our model results. This might be a result of a higher value for z_0, and thus a smaller Rossby number. Although Nicholls (1985) did not quote a mean value of α, this can be obtained from the values $A = 1.4$ and $B = 4.2$ in the drag law for neutral Ekman layers. Together with the mean values Ro = 10^9 and $u_*/G = 0.026$ for the measurements during JASIN we get $\alpha = 15°$. The data of Nicholls (1985) do not show negative values for $(u_g - u)$ between $z \sim 0.1u_*/f$ and $z \sim 0.2u_*/f$. This might be due to measuring errors because the value of

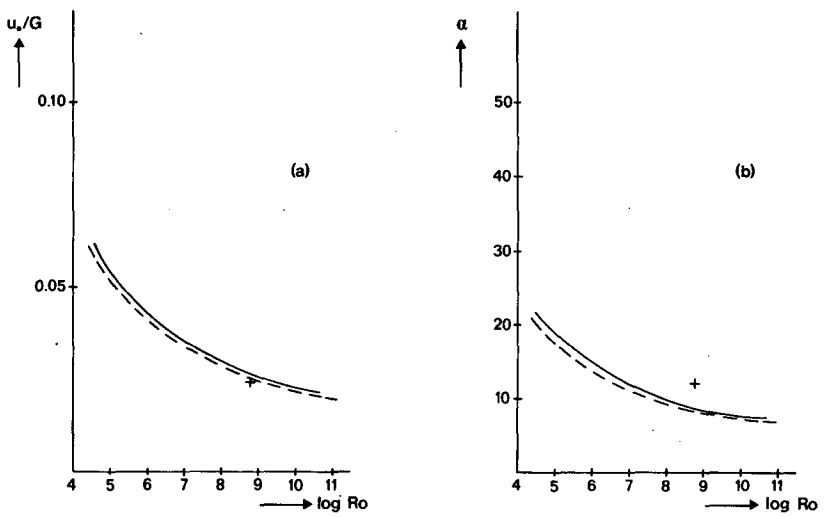

FIG. 16. (a) Geostrophic drag coefficient u_*/G and (b) cross-isobar angle α as a function of surface Rossby number (Ro); modified $E - \epsilon$ (solid); Deardorff (1972) (+); Mason and Thomson (1986) (dashed).

Unauthenticated | Downloaded 08/14/22 10:33 AM UTC

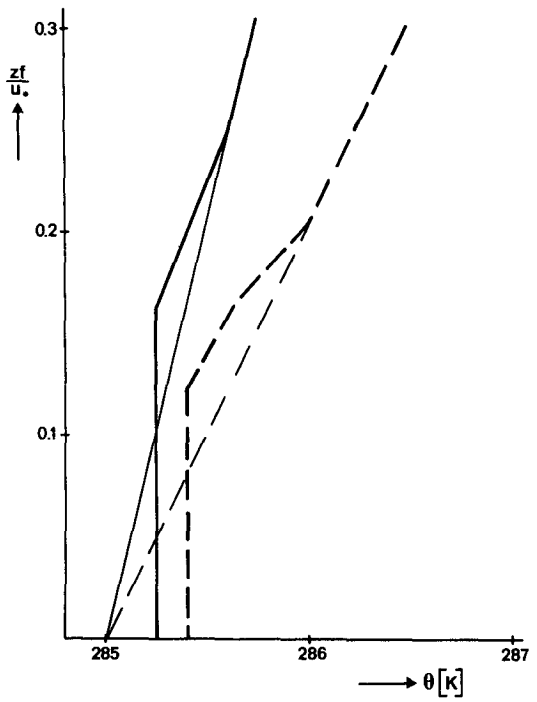

FIG. 17. The initial (thin lines) and final (thick lines) potential temperature profiles for an initial lapse rate of 1 (solid) and 2 K km^{-1} (dashed).

$\int_0^{z_i}(u_g - u)dz$ should be zero by definition (in the experimental data of Nicholls, 1985, the acceleration terms are accounted for in the definition of the geostrophic wind).

In Fig. 19 we have compared the computed stress profiles with the measured profiles of Nicholls (1985), which agree very well. The computed profiles indicate a boundary layer height of $0.2u_*/f$ and $0.16u_*/f$, respectively. Finally, the computed TKE profile is compared with the measurements of Nicholls (1985) in Fig. 20. At the top of the boundary layer, there is an abrupt drop in the calculated turbulent kinetic energy due to the stable stratification.

4. Conclusions

An $E - \epsilon$ closure model has been applied to simulate the neutral and stable atmospheric boundary layer. It is shown that the model results compare well with observations, large-eddy simulations and higher-order closure studies.

In the $E - \epsilon$ model an eddy-exchange coefficient is evaluated from the turbulent kinetic energy E and viscous dissipation ϵ. The exact equations for both E and ϵ need model assumptions. The most rigorous assumptions have to be made for the ϵ-equation. We have used the ϵ-equation in a form proposed by Lumley and Khajeb-Nouri (1974), Eq. (7).

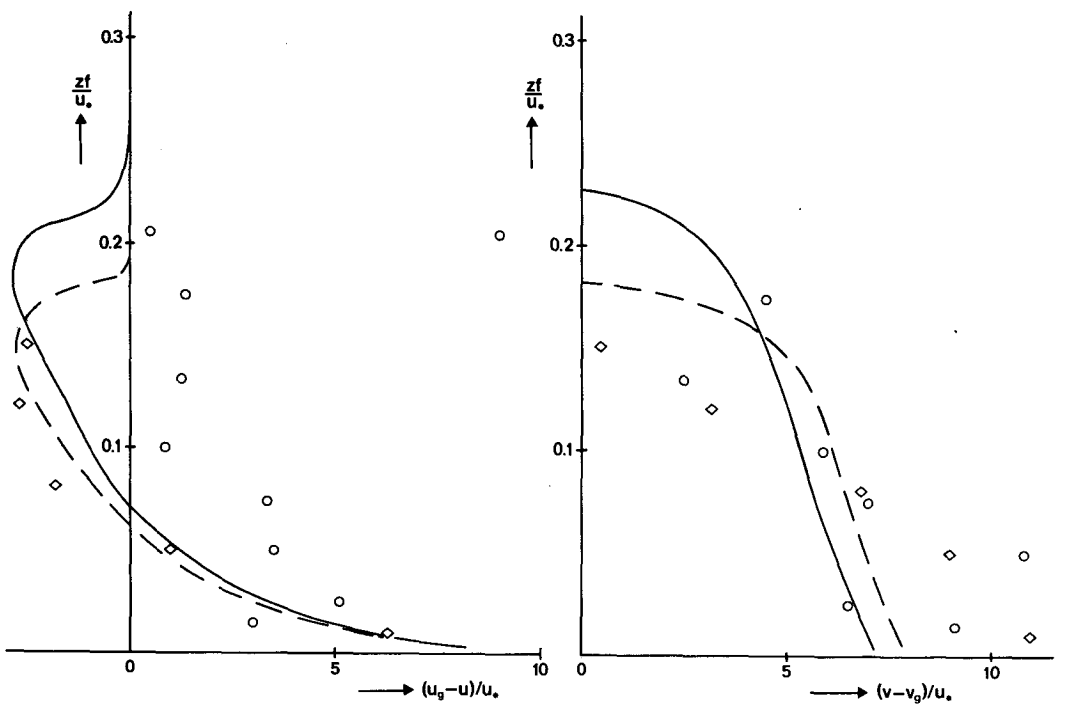

FIG. 18. Nondimensional wind defect profiles for an initial lapse rate of 1 K km^{-1} (solid) and 2 K km^{-1} (dashed) and the observational data of Nicholls (1985) (open circles) and Lettau (1950) (open diamonds).

Unauthenticated | Downloaded 08/14/22 10:33 AM UTC

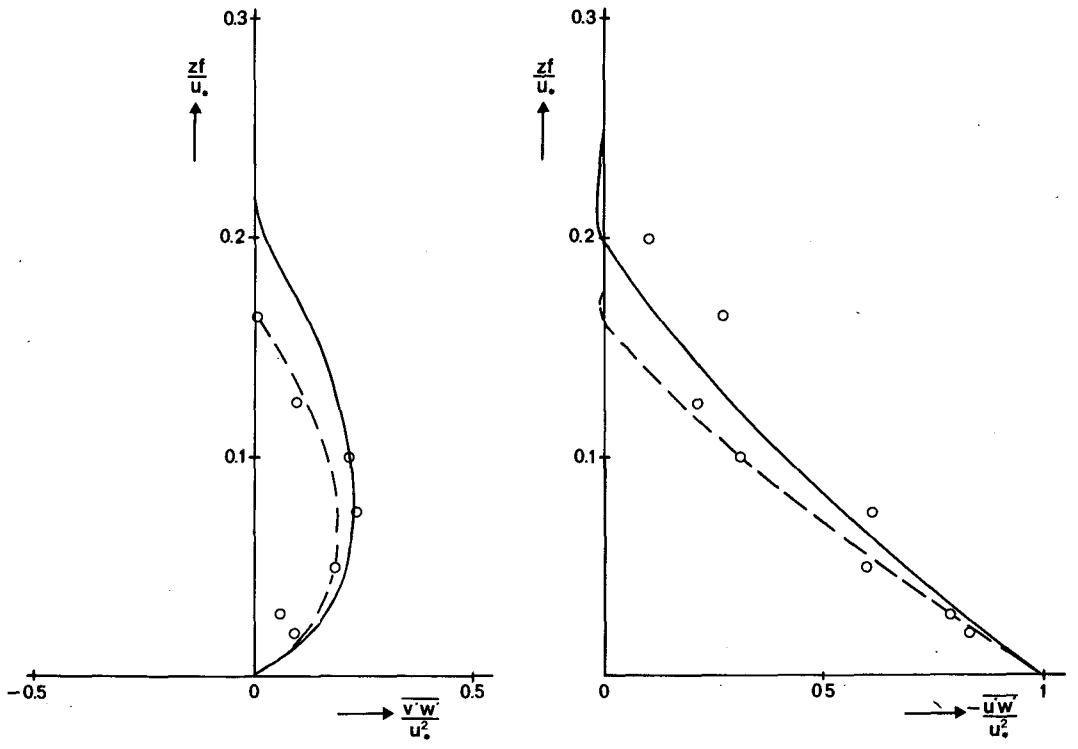

FIG. 19. Nondimensional momentum flux profiles (symbols as in Fig. 18).

Three unknown constants appear in the ϵ-equation: $c_{1\epsilon}$, $c_{2\epsilon}$ and σ_ϵ. The constant $c_{2\epsilon}$ which is connected with the destruction term is determined from the decay of grid turbulence. The value of the constant $c_{1\epsilon}$ is fixed for experiments on homogeneous shear flow (Harris et al., 1977; Tavoularis and Corrsin, 1981). The third constant σ_ϵ is determined in the surface layer in which a balance between viscous dissipation and shear production is assumed.

Besides the constants, the production term P in the ϵ-equation must be specified. Under convective conditions there is a considerable agreement to use the sum of shear production and buoyancy (Wyngaard et al., 1974). However, we showed that under stable conditions only the shear production should be included, which is nearly the same as the formulation proposed by Wyngaard (1975). Results on the neutral atmospheric boundary layer showed that the transport of turbulent kinetic energy is important and should be included in the production term P in the ϵ-equation. We included it analogous to the buoyancy term, only when it was positive (10).

For the stable atmospheric boundary layer we made a comparison with the constant cooling rate results of Wyngaard (1975) and Brost and Wyngaard (1978, 1979) and showed that our $E-\epsilon$ model can reproduce the same results. The critical Richardson behavior of the ϵ-equation is essential, i.e., as in observational data of Nieuwstadt (1983) and Garratt (1982) the model gives a constant Richardson number in the bulk of the boundary layer. We also found that the boundary layer height h obeyed Zilitinkevich's similarity prediction with

$$d = h\Big/\left(\frac{u_* L}{f}\right)^{1/2} = 0.44.$$

Comparison of model results (Deardorff, 1972; Wyngaard et al., 1974; Mason and Thomson, 1986) and observational data (Mildner, 1932; Lettau, 1950; Nicholls, 1985) on the neutral atmospheric boundary layer shows a big discrepancy between both results. For instance the model results give a boundary layer height of $h \sim 0.6u_*/f$ whereas the observations give $h \sim 0.2u_*/f$. We have shown that the observational data on the near-neutral boundary layer are in fact strongly influenced by a stable stratification. In order to do so we initialized the model with a stable lapse rate of 1 K km^{-1} and 2 K km^{-1} and set the surface heat flux to zero. From the results presented in section 3b2 it is clear that the $E-\epsilon$ model can reproduce the observations (Mildner, 1932; Lettau, 1950; Nicholls, 1985) quite well.

The model results for the neutral atmospheric boundary layer are in good agreement with both the large-eddy simulations of Deardorff (1972) and Mason and Thomson (1986) and the second-order closure

Unauthenticated | Downloaded 08/14/22 10:33 AM UTC

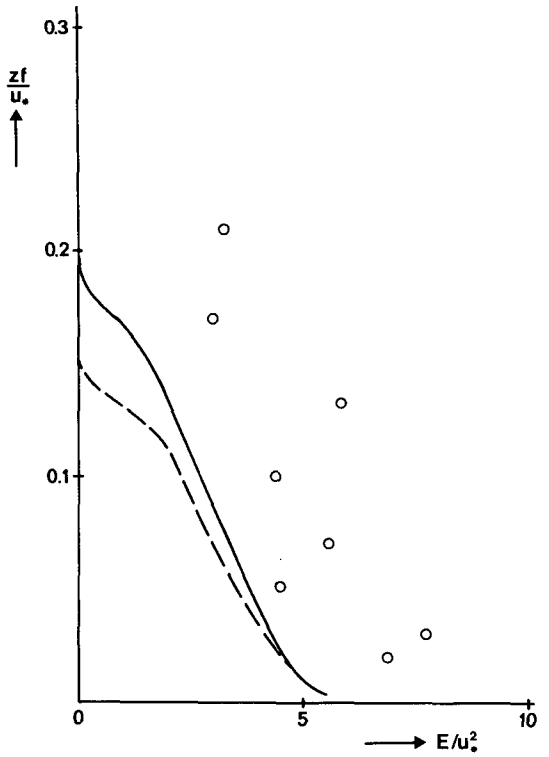

FIG. 20. Turbulent kinetic energy profile (symbols as in Fig. 18).

study of Wyngaard et al. (1974). We have shown that inclusion of the transport of turbulent kinetic energy T in the production term P of the ϵ-equation is essential in obtaining these results.

Acknowledgments. I would like to thank A. Beljaars and F. T. M. Nieuwstadt for their comments on an earlier version of this manuscript.

REFERENCES

André, J. C., G. De Moor, P. Lacarrère, G. Therry and R. du Vachat, 1978: Modeling the 24-hour evolution of the mean and turbulent structures of the planetary boundary layer. *J. Atmos. Sci.*, **35**, 1861–1883.

——, ——, ——, —— and ——, 1979: The clipping approximation and inhomogeneous turbulence simulations. *Turbulent Shear Flow I.* F. Durst, B. E. Launder, F. W. Schmidt and J. H. Whitelaw, Eds., Springer-Verlag, 307–318.

Beljaars, A. G. M., P. Schotanus and F. T. M. Nieuwstadt, 1983: Surface layer similarity under nonuniform fetch conditions. *J. Climate Appl. Meteor.*, **22**, 1800–1810.

Blackadar, A. K., 1962: The vertical distribution of wind and turbulent exchange in a neutral atmosphere. *J. Geophys. Res.*, **67**, 3095–3102.

Brost, R., and J. C. Wyngaard, 1978: A model study of the stably stratified planetary boundary layer. *J. Atmos. Sci.*, **35**, 1427–1440; 1979: Reply. *J. Atmos. Sci.*, **36**, 1821–1822.

Businger, J. A., J. C. Wyngaard, Y. Izumi and E. F. Bradley, 1971: Flux-profile relationships in the atmospheric surface layer. *J. Atmos. Sci.*, **28**, 181–189.

Deardorff, J. W., 1972: Numerical investigation of neutral and unstable planetary boundary layers. *J. Atmos. Sci.*, **29**, 91–115.

Detering, H. W., and D. Etling, 1985a: Application of the $E - \epsilon$ turbulence model to the atmospheric boundary layer. *Bound.-Layer Meteor.*, **33**, 113–133.

——, and ——, 1985b: Application of the energy-dissipation turbulence model to mesoscale atmospheric flows. *Seventh Symp. on Turbulence and Diffusion*, Boulder, Amer. Meteor. Soc., 281–284.

Duynkerke, P. G., and A. G. M. Driedonks, 1987: A model for the turbulent structure of the stratocumulus-topped atmospheric boundary layer. *J. Atmos. Sci.*, **253**, 43–64.

——, and F. T. M. Nieuwstadt, 1988: A solution of the $E - \epsilon$ model for nearly homogeneous turbulence with a mean shear. Submitted to *Appl. Sci. Res.*

Dyer, A. J., 1974: A review of flux-profile relationships. *Bound.-Layer Meteor.*, **7**, 363–372.

Fitzjarrald, D. E., 1979: On using a simplified turbulence model to calculate eddy diffusivities. *J. Atmos. Sci.*, **36**, 1817–1820.

Garratt, J. R., 1982: Observations in the nocturnal boundary layer. *Bound.-Layer Meteor.*, **22**, 24–48.

Harlow, F. H., and P. I. Nakayama, 1967: Turbulence transport equations. *Phys. Fluids*, **10**, 2323–2332.

Harris, V. G., J. A. H. Graham and S. Corrsin, 1977: Further experiments in nearly homogeneous turbulent shear flow. *J. Fluid Mech.*, **81**, 657–687.

Hinze, J. Q., 1975: Turbulence. McGraw-Hill, 790.

Lee, H. N., and S. K. Kao, 1979: Finite-element numerical modeling of atmospheric turbulent boundary layer. *J. Appl. Meteor.*, **18**, 1287–1295.

Lettau, H., 1950: A re-examination of the "Leipzig Wind Profile" considering some relations between wind and turbulence in the frictional layer. *Tellus*, **2**, 125–129.

——, 1957: Windprofil, innere Reibung und Energieumsatz in den unteren 500 m über dem Meer. *Beitr. Phys. Atmos.*, **30**, 78–96.

Lumley, J. L., and B. Khajeh-Nouri, 1974: Computational modeling of turbulent transport. *Advances in Geophysics*, Vol. 18A, Academic Press, 169–192.

Mason, P. J., and R. I. Sykes, 1980: A two-dimensional numerical study of horizontal roll vortices in the neutral atmospheric boundary layer. *Quart. J. Roy. Meteor. Soc.*, **106**, 351–366.

——, and D. J. Thomson, 1986: Large-eddy simulations of the neutral-static-stability planetary boundary layer. Submitted to *Quart. J. Roy. Meteor. Soc.*

Mildner, P., 1932: Über die Reibung in einer speziellen Luftmasse in den untersten Schichten der Atmosphäre. *Beitr. Phys. Atmos.*, **19**, 151–158.

Monin, A. S., and A. M. Yaglom, 1975: *Statistical Fluid Mechanics: Mechanics of Turbulence, Vol. 2.* J. L. Lumley, Ed., The MIT Press, 874 pp.

Nicholls, S., 1982: An observational study of the mid-latitude marine atmospheric boundary layer. PhD thesis, University of Southampton. [Available from: Department of Oceanography, Southampton SO9 5NH Hampshire, England.]

——, 1985: Aircraft observations of the Ekman layer during the Joint Air–Sea Interaction Experiment. *Quart. J. Roy. Meteor. Soc.*, **111**, 391–426.

Nieuwstadt, F. T. M., 1983: A model for the stationary, stable boundary layer. *Proc. Conf. on Models of Turbulence and Diffusion in Stably Stratified Regions of the Natural Environment*, Cambridge.

——, 1984: The turbulent structure of the stable, nocturnal boundary layer. *J. Atmos. Sci.*, **41**, 2202–2216.

Panofsky, H. A., and J. A. Dutton, 1984: *Atmospheric Turbulence.* Wiley & Sons, 397 pp.

Rao, K. S., J. C. Wyngaard and O. R. Coté, 1974: The structure of the two-dimensional internal boundary layer over a sudden change of surface roughness. *J. Atmos. Sci.*, **31**, 738–746.

Unauthenticated | Downloaded 08/14/22 10:33 AM UTC

Reynolds, W. C., 1974: Computation of turbulent flows. *AIAA Paper No. 74-556, AIAA Seventh Fluid and Plasma Dynamics Conf.,* Palo Alto. [Available from: AIAA Library, 750 3rd Avenue, New York, New York 10017.]

Rodi, W., 1980: Turbulence models and their application in hydraulics. IAHR, P.O. Box 177, 2600 MH Delft, The Netherlands.

Tavoularis, S., 1985: Asymptotic laws for transversely homogeneous turbulent shear flows. *Phys. Fluids,* **28,** 999–1001.

——, and S. Corrsin, 1981: Experiments in nearly homogeneous turbulent shear flow with a uniform mean temperature gradient. Part 1. *J. Fluid Mech.,* **104,** 311–347.

Tennekes, H., 1973: Similarity laws and scale relations in planetary boundary layers. *Workshop on Micrometeorology.* D. A. Haugen, Ed., Amer. Meteor. Soc., 177–216.

——, 1985: A comparative pathology of atmospheric turbulence in two and three dimensions. *Proc. Int. School of Physics "Enrico Fermi", Turbulence and Predictability in Geophysical Fluid Dynamics and Climate Dynamics,* North-Holland, 45–70.

——, and J. L. Lumley, 1972: *A First Course in Turbulence.* MIT Press, 300 pp.

Wyngaard, J. C., 1975: Modeling the planetary boundary layer-extension to the stable case. *Bound.-Layer Meteor.,* **9,** 441–460.

——, O. R. Coté and K. S. Rao, 1974: Modeling the atmospheric boundary layer. *Advances in Geophysics,* Vol. 18A, Academic Press, 193–211.

Zeman, O., and J. L. Lumley, 1979: Buoyancy effects in entraining turbulent boundary layers: A second-order closure study. *Turbulent Shear Flows I.* F. Durst, B. E. Launder, F. W. Schmidt and J. H. Whitelaw, Eds., Springer-Verlag, 295–306.

Unauthenticated | Downloaded 08/14/22 10:33 AM UTC